

Effective field theories for two-component repulsive bosons on lattice and their phase diagrams

Yoshihito Kuno, Keisuke Kataoka, and Ikuo Ichinose

Department of Applied Physics, Nagoya Institute of Technology, Nagoya, 466-8555 Japan

(Dated: July 9, 2018)

In this paper, we consider the bosonic t-J model, which describes two-component hard-core bosons with a nearest-neighbor (NN) pseudo-spin interaction and a NN hopping. To study phase diagram of this model, we derive effective field theories for low-energy excitations. In order to represent the hard-core nature of bosons, we employ a slave-particle representation. In the path-integral quantization, we first integrate out the radial degrees of freedom of each boson field and obtain the low-energy effective field theory of phase degrees of freedom of each boson field and an easy-plane pseudo-spin. Coherent condensates of the phases describe, e.g., a “magnetic order” of the pseudo-spin, superfluidity of hard-core bosons, etc. This effective field theory is a kind of extended quantum XY model, and its phase diagram can be investigated precisely by means of the Monte-Carlo simulations. We then apply a kind of Hubbard-Stratonovich transformation to the quantum XY model and obtain the second-version of the effective field theory, which is composed of fields describing the pseudo-spin degrees of freedom and boson fields of the original two-component hard-core bosons. As application of the effective-field theory approach, we consider the bosonic t-J model on the square lattice and also on the triangular lattice, and compare the obtained phase diagrams with the results of the numerical studies. We also study low-energy excitations rather in detail in the effective field theory. Finally we consider the bosonic t-J model on a stacked triangular lattice and obtain its phase diagram. We compare the obtained phase diagram with that of the effective field theory to find close resemblance.

PACS numbers: 67.85.Hj, 75.10.-b, 03.75.Nt

I. INTRODUCTION

In recent years, systems of cold atoms have attracted interest of many condensed-matter physicists. In particular, cold atoms put on an optical lattice sometimes regarded as a “simulator” to study canonical models of strongly correlated electron systems^{1,2}. These systems are quite controllable and impurity effects are suppressed. Systems of single-species bosonic cold atoms are described by the standard Bose-Hubbard model³, which explains the Mott-superfluid phase transition. For two-component bosonic systems, even the Mott phase exhibits rich behavior⁴. At total filling factor one and with strong inter and intra-species repulsive interactions, the two-component Bose-Hubbard model reduces to an effective spin model, i.e. Heisenberg spin model⁵, which has a nontrivial phase diagram. The experimental realization of bosonic mixture of ⁸⁷Rb -⁴¹K in a three-dimensional optical lattice is an important development⁶. The two-component Bose-Hubbard model at commensurate fillings has been studied in e.g., Refs.^{7,8} by the mean-field-theory (MFT) type approximations and the numerical methods, and its one-dimensional counterpart by the Tomonaga-Luttinger liquid theory in Ref.⁹. Phase diagrams of these systems were clarified.

From the view point of the strongly-correlated condensed matter physics, it is very interesting to study the two-component Bose-Hubbard model at *fractional fillings and with strong repulsions*. Then, we have started study of the bosonic t-J model^{10,11}, which is an effective model of the two-component Bose-Hubbard model

at the above limit and is also a kind of bosonic counterpart of the t-J model for the high- T_c superconducting phenomena¹². The bosonic t-J model (B-t-J model) describes two-component bosonic cold atoms in an optical lattice with strong inter and intra-species repulsions that can be controlled in the experiments.

Our previous studies on the B-t-J model mostly employed numerical Monte-Carlo (MC) simulations to clarify its phase diagram at finite temperature (T)¹⁰. In contrast to the fermionic t-J model, the numerical study can be done without any difficulties for some cases of the B-t-J model. In this paper, we shall derive effective fields theories of the B-t-J model and study them by both analytical and numerical methods. We mostly focus on the B-t-J model on square and triangular lattices at $T = 0$ and the phase diagram for quantum phase transitions. The obtained results are compared with the previous findings and numerical study of finite- T systems.

This paper is organized as follows. In Sec.II, we shall introduce the B-t-J model and derive first-version of an effective field theory by using the path-integral methods. The local constraint is faithfully treated by using the slave-particle representation. By integrating out amplitude modes of the slave particles, we obtained an extended quantum XY model, which describe Bose condensation of two atoms and pseudo-spin degrees of freedom. Numerical study by the Monte-Carlo (MC) methods can be performed without any difficulties and the phase diagram is obtained for the B-t-J model on both the square and triangular lattices in Sec.III. In Sec.IV, we shall derive second-version of the effective field theory from the extended quantum XY model by introducing collective

fields for the two bosons and the pseudo-spin degrees of freedom. By using this effective field theory, we obtain phase diagram of the B-t-J model and verify the consistency of the results. Furthermore we study low-energy excitations, i.e., the Nambu-Goldstone bosons in various phases in the phase diagram. In Sec.V, we numerically shall the B-t-J model in the stacked triangular lattice at finite T . Obtained phase diagram has a similar structure of the model in the triangular lattice at $T = 0$. Section VI is devoted for conclusion and discussion.

II. BOSONIC t-J MODEL AND DERIVATION OF EFFECTIVE MODEL

Hamiltonian of the B-t-J model, which will be studied in this paper, is given as^{5,10-12},

$$H_{tJ} = - \sum_{\langle i,j \rangle} t(a_i^\dagger a_j + b_i^\dagger b_j + \text{h.c.}) + J_z \sum_{\langle i,j \rangle} S_i^z S_j^z + J \sum_{\langle i,j \rangle} (S_i^x S_j^x + S_i^y S_j^y) \quad (2.1)$$

where a_i^\dagger and b_i^\dagger are boson creation operators¹³ at site i , pseudo-spin operator $\vec{S}_i = \frac{1}{2} B_i^\dagger \vec{\sigma} B_i$ with $B_i = (a_i, b_i)^t$, $\vec{\sigma}$ are the Pauli spin matrices, and $\langle i, j \rangle$ denotes nearest-neighbor (NN) sites of the lattice. We shall consider both the square and triangular lattices in the following study. Physical Hilbert space of the system consists of states with total particle number at each site less than unity (the local constraint). In order to incorporate the local constraint faithfully, we use the following slave-particle representation^{10,11},

$$a_i = \phi_i^\dagger \varphi_{i1}, \quad b_i = \phi_i^\dagger \varphi_{i2}, \quad (2.2)$$

$$\left(\phi_i^\dagger \phi_i + \varphi_{i1}^\dagger \varphi_{i1} + \varphi_{i2}^\dagger \varphi_{i2} - 1 \right) |\text{phys}\rangle = 0, \quad (2.3)$$

where ϕ_i is a boson operator that *annihilates hole* at site i , whereas φ_{1i} and φ_{2i} are bosons that represent the pseudo-spin degrees of freedom. $|\text{phys}\rangle$ is the physical state of the slave-particle Hilbert space.

The previous numerical study of the B-t-J model^{10,11,14} show that there appear various phases including superfluid with Bose condensation, state with the pseudo-spin long-range order, etc. For the most of them, the MC simulations show that density fluctuation at each lattice site is not large even in the spatially inhomogeneous states like a phase-separated state. From this observation, we expect that there appears the following term effectively,

$$H_V = \frac{V_0}{4} \sum_i \left((\varphi_{1i}^\dagger \varphi_{1i} - \rho_{1i})^2 + (\varphi_{2i}^\dagger \varphi_{2i} - \rho_{2i})^2 + (\phi_i^\dagger \phi_i - \rho_{3i})^2 \right), \quad (2.4)$$

where ρ_{1i} etc are the parameter that controls the densities of a -atom and b -atom at site i , and $V_0 (> 0)$ controls their fluctuations around the mean values. It should

be remarked here that the expectation value of the particle numbers in the physical state $|\text{phys}\rangle$ are given as $\frac{1}{N} \sum_i \langle a_i^\dagger a_i \rangle \equiv \frac{1}{N} \sum_i \text{Tr}_{\text{phys}}(a_i^\dagger a_i) = \frac{1}{N} \sum_i \text{Tr}_{\text{phys}}(\varphi_{1i}^\dagger \varphi_{1i})$ and similarly $\frac{1}{N} \sum_i \langle b_i^\dagger b_i \rangle = \frac{1}{N} \sum_i \text{Tr}_{\text{phys}}(\varphi_{2i}^\dagger \varphi_{2i})$, where N is the number of sites of the lattice and Tr_{phys} denote the trace over the states satisfying the local constraint, i.e., the physical-state condition (2.3). Therefore the constraint (2.3) requires $\sum_{\sigma=1}^3 \rho_{\sigma i} = 1$ at each site i . The values of V_0 and $\rho_{\sigma i} (\sigma = 1, 2, 3)$ are to be determined in principle by t , J_z , J and filling factor, but here we add H_V to H_{tJ} by hand and regard parameters in H_V as a free parameter. In this sense, we are considering an extended bosonic t-J model. It should be stressed here that the strong on-site repulsions between atoms enhance the effects of spatial lattice and as a result quasi-excitations with Lorentz-invariant dispersion can appear in a non-relativistic original model like the Bose-Hubbard model¹⁵.

The existence of H_V in Eq.(2.4) is very useful for study of the quantum many-particle systems. In the path-integral representation of the partition function Z , the action contains the imaginary terms like $\int d\tau \bar{\phi}_i(\tau) \partial_\tau \phi_i(\tau)$, where $\bar{\phi}_i$ is for ϕ_i^\dagger and τ is the imaginary time, i.e.,

$$Z = \int [D\phi D\varphi_1 D\varphi_2] \exp \left[- \int d\tau \left(\bar{\varphi}_{1i}(\tau) \partial_\tau \varphi_{1i}(\tau) + \bar{\varphi}_{2i}(\tau) \partial_\tau \varphi_{2i}(\tau) + \bar{\phi}_i(\tau) \partial_\tau \phi_i(\tau) + H_{tJ} + H_V \right) \right], \quad (2.5)$$

where H_{tJ} is expressed by the slave particles and the above path integral is calculated under the constraint (2.3). (In this paper we set $\hbar = 1$.) For the existence H_V , we separate the path-integral variables φ 's and ϕ as

$$\begin{aligned} \varphi_{1i} &= \sqrt{\rho_{1i} + \ell_{1i}} \exp(i\omega_{1i}), \\ \varphi_{2i} &= \sqrt{\rho_{2i} + \ell_{2i}} \exp(i\omega_{2i}), \\ \phi_i &= \sqrt{\rho_{3i} + \ell_{3i}} \exp(i\omega_{3i}), \end{aligned} \quad (2.6)$$

and we integrate out the (fluctuation of) radial degrees of freedom. There exists a constraint like $\ell_{1i} + \ell_{2i} + \ell_{3i} = 0$ on performing the path-integral over the radial degrees of freedom, i.e., $\ell_{\sigma i}$ ($\sigma = 1, 2, 3$). This constraint can be readily incorporated by using a Lagrange multiplier $\lambda_i(\tau)$,

$$\prod_\tau \delta(\ell_{1i} + \ell_{2i} + \ell_{3i}) = \int d\lambda_i e^{i \int d\tau (\ell_{1i} + \ell_{2i} + \ell_{3i}) \lambda_i}.$$

The variables $\ell_{\sigma i}$ ($\sigma = 1, 2, 3$) also appear in H_{tJ} , but we ignore them by simply replacing $\varphi_{\sigma i} \rightarrow \sqrt{\rho_{\sigma i}} \exp(i\omega_{\sigma i})$, and then we have

$$\begin{aligned} & \int d\lambda_i d\ell_i e^{\int d\tau \sum_{\sigma=1}^3 (-V_0 (\ell_{\sigma i})^2 + i\ell_{\sigma i} (\partial_\tau \omega_{\sigma i} + \lambda_i))} \\ &= \int d\lambda_i e^{-\frac{1}{4V_0} \int d\tau \sum_\sigma (\partial_\tau \omega_{\sigma i} + \lambda_i)^2}, \end{aligned} \quad (2.7)$$

where we have ignored the terms like $\int d\tau \partial_\tau \omega_{\sigma,i}$ by the periodic boundary condition for the imaginary time. The resultant quantity on the RHS of (2.7) is positive definite, and therefore the numerical study by the MC simulation can be done without any difficulty. It should be remarked that the Lagrange multiplier λ_i in Eq.(2.7) behaves as a gauge field, i.e., the RHS of (2.7) is invariant under the following ‘‘gauge transformation’’, $\omega_{\sigma,i} \rightarrow \omega_{\sigma,i} + \alpha_i$, $\lambda_i \rightarrow \lambda_i - \partial_\tau \alpha_i$. In the practical calculation, we shall show that all physical quantities are invariant under the above gauge transformation.

Various phases can form in the system (2.1) at $T = 0$, e.g., states with long-range spin orders (FM, AF, spiral, etc), superfluid with Bose condensation of a and/or b atoms, and superposition of them (the supersolid (SS))^{7,8,14,16}. In the following sections, we shall consider several specific cases of the extended B-t-J model $H_{tJ} + H_V$ and derive effective field-theory model. Then we clarify the phase diagram of the B-t-J model by studying the effective model.

III. PHASE DIAGRAM OF THE EXTENDED QUANTUM XY MODEL: NUMERICAL STUDY

A. FM coupling on square lattice

In this section, we shall study the effective field theory obtained in the previous section on the two-dimensional (2D) square lattice as the first example. One of the simplest case is xy -FM system corresponding to $J_z = 0$ and $J < 0$ in Eq.(2.1), though an extension to the case $|J_z| < -J$ is rather straightforward. In this case the pseudo-spin symmetry is $O(2)$, and then we put $\rho_{1i} = \rho_{2i} = \rho$ and $\rho_{3i} = 1 - 2\rho$. The partition function Z_{qXY} of the effective theory is obtained as follows from Eqs.(2.5) and (2.7),

$$Z_{\text{qXY}} = \int \left[\prod_{\sigma=1,2,3} D\omega_\sigma \right] \exp \left[-A_\tau - A(e^{i\Omega_\sigma}, e^{-i\Omega_\sigma}) \right], \quad (3.1)$$

where

$$\begin{aligned} A_\tau &= \frac{1}{4V_0} \int d\tau \sum_{i,\sigma} (\partial_\tau \omega_{\sigma,i} + \lambda_i)^2, \\ A(e^{i\Omega_\sigma}, e^{-i\Omega_\sigma}) &= \int d\tau \left[\right. \\ &- \sum_{\langle i,j \rangle} c_h \left(\cos(\Omega_{2,i} - \Omega_{2,j}) + \cos(\Omega_{3,i} - \Omega_{3,j}) \right) \\ &\left. - c_s \sum_{\langle i,j \rangle} \cos(\Omega_{1,i} - \Omega_{1,j}) \right] \end{aligned} \quad (3.2)$$

where

$$\Omega_{1i} = \omega_{1i} - \omega_{2i}, \quad \Omega_{2i} = \omega_{1i} - \omega_{3i}, \quad \Omega_{3i} = \omega_{2i} - \omega_{3i},$$

and

$$c_h = \frac{t}{2} \rho (1 - 2\rho), \quad c_s = 4J\rho^4. \quad (3.3)$$

It is obvious that the integrand in Eq.(3.1) is positive definite, and therefore the numerical calculation of Z_{qXY} by means of the MC simulation is possible without any difficulty. The model (3.1) is a kind of lattice rotor model.

For practical calculation, we introduce a lattice for the imaginary-time direction and use the following lattice action $A_{L\tau}$ corresponding to A_τ

$$A_{L\tau} = c_\tau \sum_r \sum_{\sigma=1}^3 \cos(\omega_{\sigma,r+\hat{\tau}} - \omega_{\sigma,r} + \lambda_r), \quad (3.4)$$

where r denotes site of the space-time cubic lattice, $c_\tau = \frac{1}{V_0 \Delta\tau}$ and $\Delta\tau$ is the lattice spacing of the imaginary-time direction.

We numerically studied the lattice model defined by the lattice action

$$A_{L\text{XY}} = A_{L\tau} + A_L(e^{i\Omega_\sigma}, e^{-i\Omega_\sigma}), \quad (3.5)$$

where $A_L(e^{i\Omega_\sigma}, e^{-i\Omega_\sigma})$ corresponds to $A(e^{i\Omega_\sigma}, e^{-i\Omega_\sigma})$ in Eq.(3.2),

$$\begin{aligned} A_L(e^{i\Omega_\sigma}, e^{-i\Omega_\sigma}) &= \\ &- \sum_{\langle r,r' \rangle} C_3 \left(\cos(\Omega_{2,r} - \Omega_{2,r'}) + \cos(\Omega_{3,r} - \Omega_{3,r'}) \right) \\ &- C_1 \sum_{\langle r,r' \rangle} \cos(\Omega_{1,r} - \Omega_{1,r'}), \end{aligned} \quad (3.6)$$

where $C_1 = c_s \Delta\tau$ and $C_3 = c_h \Delta\tau$, and $\langle r, r' \rangle$ denotes the NN sites in the 2D spatial lattice. Here it is helpful to notice that the parameters $C_1 \propto J/V_0$ and $C_3 \propto t/V_0$ are dimensionless. We fixed the value of the dimensionless parameter c_τ and calculated the partition function Z , the ‘‘internal energy’’ E and ‘‘specific heat’’ C as a function of C_1 and C_3 ,

$$\begin{aligned} Z &= \int [d\omega] e^{-A_{L\text{XY}}}, \\ E &= \langle A_{L\text{XY}} \rangle / L^3, \\ C &= \langle (A_{L\text{XY}} - E)^2 \rangle / L^3, \end{aligned} \quad (3.7)$$

where L is the linear size of the 3D cubic lattice. In order to identify various phases, we also calculated the following pseudo-spin and boson correlation functions,

$$\begin{aligned} G_S(r) &= \frac{1}{L^3} \sum_i \langle e^{i\Omega_{1,i}} e^{-i\Omega_{1,i+r}} \rangle, \\ G_a(r) &= \frac{1}{L^3} \sum_i \langle e^{i\Omega_{2,i}} e^{-i\Omega_{2,i+r}} \rangle, \\ G_b(r) &= \frac{1}{L^3} \sum_i \langle e^{i\Omega_{3,i}} e^{-i\Omega_{3,i+r}} \rangle, \end{aligned} \quad (3.8)$$

where sites i and $i+r$ are located in the same spatial 2D lattice, i.e., the equal-time correlations. For example, $G_a(r) \rightarrow \text{finite}$ as $r \rightarrow \infty$ indicates Bose-Einstein condensation (BEC) of the a -atom.

For numerical simulations, we employ the standard Monte-Carlo Metropolis algorithm with local update¹⁷.

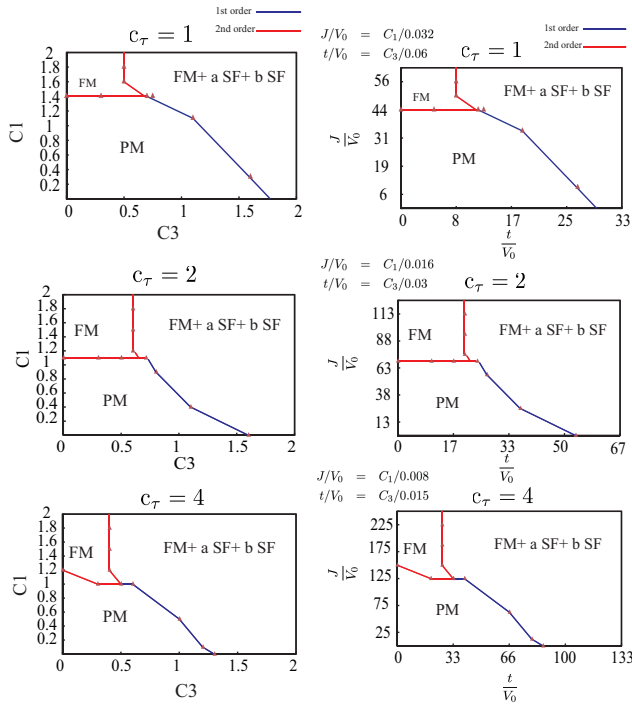


FIG. 1. (Color online) Phase diagram of the effective field theory A_{LXY} on 3D cubic lattice for various values of c_τ . $\rho = 0.35$. Dots denote the observed phase transition point. Thick line denotes first-order phase transition line whereas the others are second-order transition lines. System size $L = 24$.

$C1=0.4$ ($J/V_0 = 9.1$)

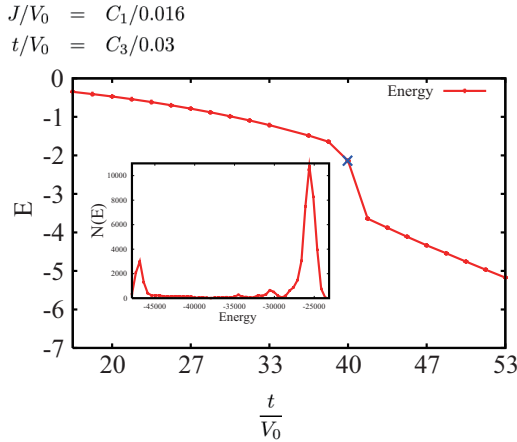


FIG. 2. (Color online) Internal energy E and density of state $N(E)$ for the phase transitions shown in Fig.1. Double-peak shape for $\frac{J}{V_0} = 9.1$ and $\frac{t}{V_0} = 40.0$ indicates first-order phase transition. $c_\tau = 2$ and $L = 24$.

The typical sweeps for measurement is $(30000 \sim 50000) \times$ (10 samples), and the acceptance ratio is 40% \sim 50%. Errors are estimated from 10 samples with the jackknife methods.

We numerically studied the model with the system size $L = 14, 16, 20, 24, 28$ and show the obtained phase dia-

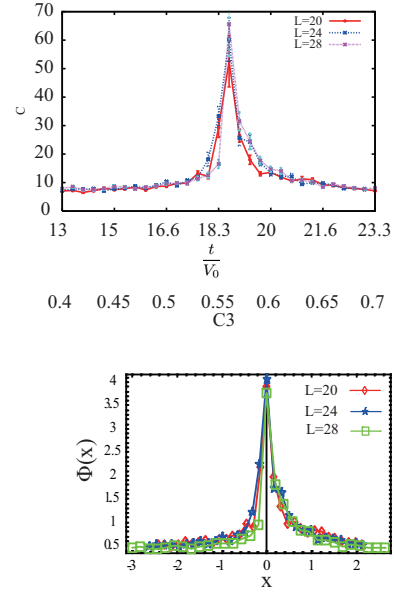


FIG. 3. (Color online) Specific heat C and its finite-size scaling function $\Phi(x)$ for the second-order phase transition shown in Fig.1. $c_\tau = 2$ and $\frac{J}{V_0} = 87.5$ ($C_1 = 1.4$).

gram for $\rho = 0.35$ in Fig.1 using $L = 24$ data. There are three phases and they are separated with each other by first or second-order phase transition lines. To identify the first-order phase transition, we calculated the “density of state” $N(E)$ defined by

$$N(E)\Delta E = \text{Number of configurations with}$$

$$A_{LXY} = (E + \Delta E) \sim E. \quad (3.9)$$

Step function like behavior of E and double-peak shape of $N(E)$ at the critical point indicate the existence of a first-order phase transition. We show some of the results in Fig.2. On the other hand to identify second-order phase transition, we used nonsingular behavior of E , single-peak shape of $N(E)$ and system-size dependence of the specific heat C in Eq.(3.7). For example, see Fig.3. System-size dependence of the specific heat is parameterized as follows,

$$C_L(\epsilon) = L^{\sigma/\nu} \Phi(L^{1/\nu} \epsilon), \quad (3.10)$$

where ν and σ are critical exponents, $\epsilon = (C_3 - C_{3\infty})/C_{3\infty}$ with $C_{3\infty} =$ the critical coupling of $L \rightarrow \infty$, and $\Phi(x)$ is the scaling function. Estimated values are $\nu = 1.35$, $\sigma = 1.2$ and $C_{3\infty} = 0.56$ ($\frac{t}{V_0} = 19$).

From Fig.1, it is obvious that for small t and J , there exists a “paramagnetic state” (PM state) without any long-range orders (LRO’s) and its domain in the $c_3 - c_1$ plane is decreased for increasing c_τ . In this PM state, a superposition of a -atom and b -atom is realized at each site, but coherence of the relative phase in the superposition does not exist. It should be notice that the atomic BEC always accompanies the pseudo-spin LRO. The obtained results are in good agreement with the result of

the previous study on some related model on 3D cubic lattice at finite T^{11} .

B. AF coupling on triangular lattice

In this subsection, we shall study the B-t-J model on the 2D triangular lattice. As we also discretize the imaginary time, the model A_{LXY} in Eq.(3.5) is defined on the 3D stacked triangular lattice. In this section we consider the case of the xy -AF case with $O(2)$ symmetry. Therefore we set $J > 0$ and $J_z = 0$ in Eq.(2.1). As there exists the frustration, we expect that various phases appear in contrast to the xy -FM case. In later section, we also show the result of the numerical study of the B-t-J model on the stacked triangular lattice *at finite but low T* , which is closely related to the 2D model at $T = 0$. This close relation between 3D model at low T and 2D model at $T = 0$ has been previously observed in various systems¹⁸. Origin of this similarity is somewhat obvious from $A_{L\tau}$ in Eq.(3.4) as it can be regarded as an inter-layer coupling.

To perform the numerical calculation, we first assign values of the parameters ρ_{1i}, ρ_{2i} ($\rho_{3i} = 1 - \rho_{1i} - \rho_{2i}$). Here we assume a homogeneous state and put $\rho_{1i} = \rho_{2i} = \rho$ ($\rho_{3i} = 1 - 2\rho$) as in the previous case. Results of more general cases will be reported in a future publication.

We numerically studied the system on the triangular lattice for the system size $L = 12, 14$ and 18 . In Fig.4, we show the obtained phase diagram for $\rho = 0.3$ and the hole density = 0.4. Order of the phase transitions were determined as in the case of the FM coupling on the square lattice. There are six phases in the $t - J$ plane, and the order of the phase transitions was determined as in the case of the square lattice. For small t (i.e., small C_3), the pseudo-spin degrees of freedom exhibits the 120° long-range order. As we assume a homogeneous hole distribution, a superposed state of atoms and hole is realized at each site, but coherent condensation of atoms does not take place yet. As t is increased, phase transition to the states with the 120° long-range order and Bose condensation take place. For example in the phase B in Fig.4, the both atoms Bose condense, as the correlation functions shown in Fig.5 exhibit. In the mean-field approximation, the wave function of that state is given by

$$\begin{aligned}
 |\Psi\rangle = & \prod_{i \in A} [a_i^\dagger + b_i^\dagger + c_A] \\
 & \times \prod_{i \in B} [a_i^\dagger + e^{i\frac{2\pi}{3}} b_i^\dagger + c_B] \\
 & \times \prod_{i \in C} [a_i^\dagger + e^{-i\frac{2\pi}{3}} b_i^\dagger + c_C] |0\rangle,
 \end{aligned}$$

where c 's are some complex number and $|0\rangle$ is the empty state of a and b -atoms. This phase will be discussed by using the effective field theory in Sec.IV.C and also by the MC simulations in Sec.V. As the parameter C_3 is increased further, order of the pseudo-spin is destroyed

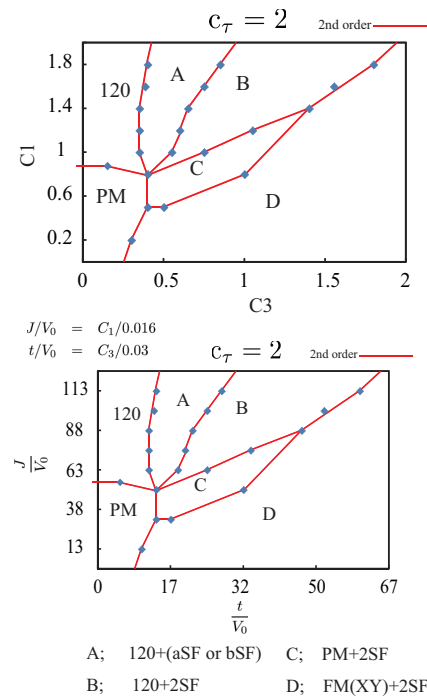


FIG. 4. (Color online) Phase diagram of the quantum XY model on triangular lattice. Density of each boson $\rho = 0.3$. System size $L = 18$. There are six phases. Phase of 120° denotes the state with 120° pseudo-spin long-range order without atomic BEC. SF stands for superfluid.

first (phase C) and then changes to the FM one in the $S^x - S^y$ plane (phase D).

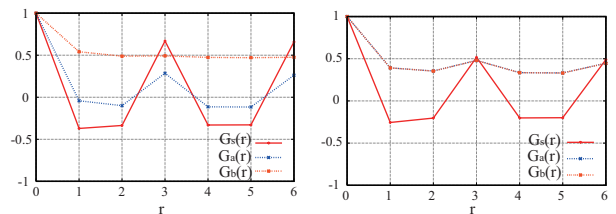


FIG. 5. (Color online) Correlation functions in the phase diagram. $t/V_0 = 21.7$ ($C_3 = 0.65$) and $J/V_0 = 100$ ($C_1 = 1.6$) (left), $t/V_0 = 33.3$ ($C_3 = 1.0$) and $J/V_0 = 100$ ($C_1 = 1.6$) (right). $L = 12$.

IV. EFFECTIVE FIELD THEORY FOR BOSE CONDENSATION AND PSEUDO-SPIN ORDER

In the previous sections, we numerically studied lattice quantum XY model that describe the two-component bosons with strong repulsions. The obtained phase diagrams show that there exist Bose-condensed phases as well as the state of simple pseudo-spin LRO. In this section, we shall derive an effective field theory from the quantum XY model, which describes directly the Bose condensation and spin order. This field theory not only

explains the numerically obtained phase diagram but also reveals low-energy excitations and interactions between them. This kind of effective field theory has been obtained and discussed for a granular superfluid etc by using Hubbard-Stratonovichi transformation¹⁹. In this section we shall employ a slightly different method²⁰. As a result, we reveal some important point that has been overlooked so far.

A. Effective field theory

To illustrate the procedure to derive the effective field theory, we first consider a single rotor model as an example that describes superfluid phase transition. After consideration of the simple model, we shall apply similar methods to the quantum XY model for the B-t-J model.

We first rewrite the partition function of the rotor model on the square lattice by introducing source terms,

$$\begin{aligned} Z_{\text{rotor}} &= \int [d\omega] e^{-\frac{1}{V_0} \int d\tau \sum \dot{\omega}_i^2 - \int d\tau H(e^{i\omega_i}, e^{-i\omega_i})} \\ &= \int [d\omega] e^{-\frac{1}{V_0} \int d\tau \sum \dot{\omega}_i^2 - \int d\tau H(\frac{\delta}{\delta \eta_i}, \frac{\delta}{\delta \bar{\eta}_i})} \\ &\quad \times I(\eta_i, \omega_i)|_{\eta=\bar{\eta}=0}, \end{aligned} \quad (4.1)$$

$$I(\eta_i, \omega_i) = e^{\int d\tau \sum (\eta_i e^{i\omega_i} + \bar{\eta}_i e^{-i\omega_i})}, \quad (4.2)$$

where $\dot{\omega}_i = \partial_\tau \omega_i$ and

$$H(e^{i\omega_i}, e^{-i\omega_i}) = -J \sum_{\langle i,j \rangle} \cos(\omega_i - \omega_j).$$

In Eq.(4.1), we evaluate the path integral of ω_i as

$$\begin{aligned} &\int [d\omega] e^{-\frac{1}{V_0} \int d\tau \sum \dot{\omega}_i^2} I(\eta_i, \omega_i) \\ &= e^{\int d\tau \int d\tau' \bar{\eta}_i(\tau) e^{-V_0 |\tau - \tau'|} \eta_i(\tau')}, \end{aligned} \quad (4.3)$$

where we have used

$$\langle e^{i\omega_i(\tau)} e^{-i\omega_i(\tau')} \rangle = e^{-V_0 |\tau - \tau'|}, \quad (4.4)$$

and the fact that other correlators like $\langle e^{i\omega_i(\tau)} e^{i\omega_i(\tau')} \rangle$ are vanishing. RHS of Eq.(4.3) can be expressed by introducing a complex boson field Φ_i as

$$\begin{aligned} &e^{\int d\tau \int d\tau' \bar{\eta}_i(\tau) e^{-V_0 |\tau - \tau'|} \eta_i(\tau')} \\ &= \int [d\Phi] \exp \left[-\frac{1}{V_0} \int d\tau \Phi_i^* (-\partial_\tau^2 + V_0^2) \Phi_i \right. \\ &\quad \left. + \int d\tau (\eta_i \Phi_i + \bar{\eta}_i \Phi_i^*) \right]. \end{aligned} \quad (4.5)$$

By inserting Eq.(4.5) into Eq.(4.1), we obtain the effective field theory of the rotor model with the following

action A_{rotor} ,

$$\begin{aligned} A_{\text{rotor}} &= \int d\tau \left[\frac{1}{V_0} \sum_i \Phi_i^* (-\partial_\tau^2 + V_0^2) \Phi_i \right. \\ &\quad \left. - \frac{J}{2} \sum_{\langle i,j \rangle} (\Phi_i^* \Phi_j + \text{c.c.}) \right], \\ Z_{\text{rotor}} &= \int [d\Phi] e^{-A_{\text{rotor}}}. \end{aligned} \quad (4.6)$$

The above derivation from Eq.(4.1) to Eq.(4.6) seems exact because the integration of $\omega_i(\tau)$ is the one-site integral and essentially Gaussian integration of the free fields. In fact the above manipulation is exact as long as the boson field Φ_i does not Bose condense. On the other hand for $J \gg V_0$, the Bose condensation of Φ_i takes place, i.e., $\langle \Phi_i \rangle \neq 0$. One may wonder if the above manipulation is applicable even for this case because Eq.(4.4) seems to indicate *nonexistence* of the long-range order of Φ_i . Furthermore in this case, the mass term of Φ_i becomes negative, and the integration of Φ_i in Eq.(4.6) becomes unstable, e.g., for the square lattice

$$\begin{aligned} &\frac{J}{2} \sum_{i,\mu} (\Phi_i^* \Phi_{i+\mu} + \text{c.c.}) - V_0 \sum_i |\Phi_i|^2 \\ &= -\frac{J}{2} \sum_{i,\mu} |\nabla_\mu \Phi_i|^2 + \sum_i (zJ - V_0) |\Phi_i|^2, \end{aligned} \quad (4.7)$$

where ∇_μ is the lattice difference operator and z is the number of links emanating from a single site and $z = 4$ for the square lattice. This instability comes from the fact that the order of the η -derivative and the ω -integration is *not interchangeable* when the Bose condensation, i.e., a phase transition to an ordered state, takes place. It is obvious $\langle \Phi_i \rangle = \langle e^{i\omega_i} \rangle < 1$ in the Bose condensed state, and therefore it is plausible to expect term like $\lambda |\Phi_i|^4$ to appear in the effective field theory to stabilize the integration of Φ_i for the Bose condensed state, though explicit calculation to determine the coefficient is difficult. Simple spin-wave like approximation for the rotor model,

$$J \cos(\omega_i - \omega_j) \sim J - \frac{J}{2} (\omega_i - \omega_j)^2,$$

gives the estimation like $\langle e^{i\omega_i} \rangle \langle e^{-i\omega_i} \rangle \sim e^{-\frac{V_0}{J}}$, and then the coefficient of the $|\Phi_i|^4$ -term is estimated as $\lambda \sim J e^{\frac{V_0}{J}}$ for $J \gg V_0$.

Hubbard-Stratonovichi transformation derives a similar effective field theory to the above. But its straightforward application gives a negative coefficient of the $|\Phi_i|^4$ -term indicating an instability of the system. This means that certain step of the derivation is invalid, e.g., introduction of the Hubbard-Stratonovichi field and the ω -integration is not interchangeable. This problem is under study and the result will be reported in a separate publication.

Similar manipulation to the above can be applied to the present quantum extended XY model. From

Eqs.(3.1) and (3.2),

$$\begin{aligned}
Z_{\text{qXY}} &= \int [d\omega] e^{-\frac{1}{V_0} \int d\tau \dot{\omega}_{\sigma i}^2 - A(e^{i\Omega_{\sigma i}}, e^{-i\Omega_{\sigma i}})} \\
&= \int [d\omega] e^{-\frac{1}{V_0} \int d\tau \sum \dot{\omega}_{\sigma i}^2 - A(\frac{\delta}{\delta \eta_{\sigma i}}, \frac{\delta}{\delta \bar{\eta}_{\sigma i}})} \\
&\quad \times I(\eta_{\sigma i}, \Omega_{\sigma i})|_{\eta=\bar{\eta}=0}, \\
I(\eta_{\sigma i}, \Omega_{\sigma i}) &= e^{\int d\tau \sum (\eta_{\sigma i} e^{i\Omega_{\sigma i}} + \bar{\eta}_{\sigma i} e^{-i\Omega_{\sigma i}})}, \quad (4.8)
\end{aligned}$$

where $\dot{\omega}_{\sigma i} = \partial_{\tau} \omega_{\sigma i}$ and we have omitted the gauge field λ_i as we consider the only gauge-invariant objects through $\Omega_{\sigma i}$. Then the integration over $\omega_{\sigma i}$ can be performed as,

$$\int [d\omega] e^{-\frac{1}{V_0} \int d\tau \sum_{\sigma} \dot{\omega}_{\sigma i}^2} I(\eta_{\sigma i}, \Omega_{\sigma i}) = \tilde{I}(\eta_{\sigma i}, \bar{\eta}_{\sigma i}), \quad (4.9)$$

and the Green function of $\omega_{\sigma i}(\tau)$, G_{ω} , is obtained as

$$\langle e^{i\omega_{\sigma i}(\tau)} e^{-i\omega_{\sigma' i}(\tau')} \rangle = \delta_{\sigma\sigma'} e^{-V_0 |\tau - \tau'|}. \quad (4.10)$$

Typical term of $\tilde{I}(\eta_{\sigma i}, \bar{\eta}_{\sigma i})$ is as follows,

$$e^{\int d\tau \int d\tau' \bar{\eta}_{\sigma i}(\tau) e^{-2V_0 |\tau - \tau'|} \eta_{\sigma i}(\tau')},$$

and this quantity is expressed by introducing complex scalar fields $\Phi_{\sigma i}(\tau)$ as

$$\begin{aligned}
&e^{\int d\tau \int d\tau' \bar{\eta}_{\sigma i}(\tau) e^{-2V_0 |\tau - \tau'|} \eta_{\sigma i}(\tau')} \\
&= \int [d\Phi] \exp \left[-\frac{1}{4V_0} \int d\tau \Phi_{\sigma i}^* (-\partial_{\tau}^2 + 4V_0^2) \Phi_{\sigma i} \right. \\
&\quad \left. + \int d\tau (\eta_{\sigma i} \Phi_{\sigma i} + \bar{\eta}_{\sigma i} \Phi_{\sigma i}^*) \right]. \quad (4.11)
\end{aligned}$$

By inserting $\tilde{I}(\eta_{\sigma i}, \bar{\eta}_{\sigma i})$, which is expressed in terms of the boson fields $\Phi_{\sigma i}(\tau)$ for $e^{i\Omega_{\sigma i}}$, into Eq.(4.8), the action of the effective field theory is obtained as follows,

$$\begin{aligned}
A_0 &= \int d\tau \left[\sum_{\sigma, (i,j)} (a_{\sigma} \Phi_{\sigma i}^* \Phi_{\sigma j}) - \frac{1}{4V_0} \sum_{\sigma i} (|\dot{\Phi}_{\sigma i}|^2 + 4V_0^2 |\Phi_{\sigma i}|^2) \right. \\
&\quad \left. + \sum_i g (\Phi_{1i}^* \Phi_{2i} \Phi_{3i}^* + \text{c.c.}) \right], \quad (4.12)
\end{aligned}$$

where $a_1 = a_s$, $a_2 = a_3 = a_h$ and $g = \frac{3}{2V_0^2}$. To describe the Bose condensed state, we add the $|\Phi|^4$ -terms in the effective field theory and discuss the phase diagram of the system. The final form of the effective action is therefore given by

$$\begin{aligned}
A_{\text{eff}} &= A_0 - \int d\tau \sum_{\sigma, i} (\lambda_{\sigma} |\Phi_{\sigma i}|^4) \\
&= \int d\tau L_{\text{eff}}, \\
Z &= \int [d\Phi] e^{-A_{\text{eff}}}. \quad (4.13)
\end{aligned}$$

$$\begin{aligned}
V &= \lambda_1 |\Phi_1|^4 + 2\lambda_2 |\Phi_2|^4 \\
&\quad + \lambda_3 |\Phi_1|^2 + 2\lambda_4 |\Phi_2|^2 - g |\Phi_1| |\Phi_2|^2
\end{aligned}$$

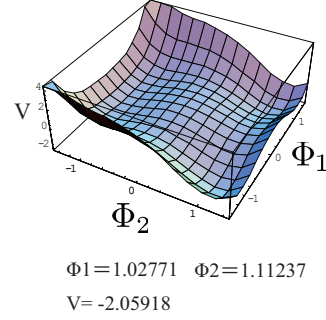


FIG. 6. (Color online) Potential $V(\Phi_{\sigma})$ (4.14) and its minimum. Symmetric case $\Phi_2 = \Phi_3$. Parameters are $\lambda_1 = 1$, $\lambda_2 = \frac{1}{2}$, $\lambda_3 = -1$, $\lambda_4 = -1$, and $g = 1$.

B. Phase diagram and low-energy excitations: Square lattice

In this subsection, we shall apply the field-theoretical approach explained in the previous subsection to the B-t-J model on the square lattice as a simple example. Furthermore we focus on the FM parameter region $J < 0$. In this case there exists no frustration and therefore it is rather straightforward to obtain the phase diagram. Nevertheless study on this system reveals important aspect of the state with multiple long-range orders and structure of the Nambu-Goldstone bosons.

This system was studied in Sec.III.A, and we obtained the phase diagram by MC simulations. The potential $V(\Phi_{\sigma})$ of the present system is given as follows from the effective field theory in Sec.IV.A,

$$\begin{aligned}
V(\Phi_{\sigma}) &= \sum_{\sigma} (V_0 - 2za_{\sigma}) |\Phi_{\sigma}|^2 - g (\Phi_1^* \Phi_2 \Phi_3^* + \text{c.c.}) \\
&\quad + \sum_{\sigma} \lambda_{\sigma} |\Phi_{\sigma}|^4. \quad (4.14)
\end{aligned}$$

From the first term of Eq.(4.14), it is obvious that spontaneous symmetry breaking occurs for $a_{\sigma} > V_0$, but the second terms that represent the interplay between the order parameters give nontrivial contribution to the phase diagram. In Fig.6, we show typical potential and its minimum obtained from Eq.(4.14), which derives qualitatively the same phase structure with that obtained in Sec.III.A.

It is interesting to see how gapless low-energy excitations, i.e., Nambu-Goldstone (NG) bosons, appear in the present system. In the phase with the FM spin order $\langle \Phi_3 \rangle = v > 0$, we set $\Phi_{3i} = v + \psi_i + i\chi_i$, and then it is obvious that the field χ_i describes a NG boson that appears as a result of the spontaneous symmetry breaking of the U(1) pseudo-spin symmetry.

Interesting point is that how many NG bosons appear in the phase with the FM+2SF. If $g = 0$ in Eq.(4.12), it is obvious that there exist three NG bosons. However in the

original B-t-J model, the symmetry is $U(1) \times U(1)$ for the global phase rotation of a and b -boson operators. In order to study the low-energy excitations in the effective field theory, we shall take the continuum description instead of the lattice one though it is not essential.

For the FM B-t-J model on the square lattice, it is straightforward to derive effective Lagrangian L_{eff} in the continuum spacetime from the effective field theory on the lattice. For example in Eq.(4.12), we put

$$\begin{aligned} & \sum_{i,\mu} \Phi_i^* \Phi_{i+\mu} + \Phi_i \Phi_{i+\mu}^* \\ &= - \sum_{i,\mu} |\nabla_\mu \Phi_i|^2 + \sum_i 2z |\Phi_i|^2 \\ &\Rightarrow - \sum_{i,\mu} |\partial_\mu \Phi_i|^2 + \sum_i 2z |\Phi_i|^2. \end{aligned}$$

Then L_{eff} in the continuum is derived as follows from Eq.(4.13)

$$\begin{aligned} L_{\text{eff}}^{\text{sq}} &= \left(a_s |\nabla \Phi_1(x)|^2 + a_h |\nabla \Phi_2(x)|^2 + a_h |\nabla \Phi_3(x)|^2 \right) \\ &- \left(\frac{1}{4V_0} |\partial_\tau \Phi_1(x)|^2 + \frac{1}{4V_0} |\partial_\tau \Phi_2(x)|^2 \right. \\ &\left. + \frac{1}{4V_0} |\partial_\tau \Phi_3(x)|^2 \right) + V(\Phi_\sigma), \end{aligned} \quad (4.15)$$

where the potential $V(\Phi_\sigma)$ is given as

$$\begin{aligned} V(\Phi_\sigma) &= (V_0 - 2za_s) |\Phi_1(x)|^2 + (V_0 - 2za_h) |\Phi_2(x)|^2 \\ &+ (V_0 - 2za_h) |\Phi_3(x)|^2 \\ &- g(\Phi_1^*(x)\Phi_2(x)\Phi_3^*(x) + \text{c.c.}) \\ &+ \lambda_1 |\Phi_1(x)|^4 + \lambda_2 |\Phi_2(x)|^4 + \lambda_3 |\Phi_3(x)|^4. \end{aligned} \quad (4.16)$$

We first substitute

$$\Phi_1(x) = \sqrt{n_0}, \quad \Phi_2(x) = \sqrt{n_1}, \quad \Phi_3(x) = \sqrt{n_1}$$

into $V(\Phi_\sigma)$,

$$\begin{aligned} V(n_0, n_1) &= \lambda_1 n_0^2 + 2\lambda_2 n_1^2 + \lambda_4 n_0 + 2\lambda_5 n_1 \\ &- 2g\sqrt{n_0 n_1}, \end{aligned} \quad (4.17)$$

and derive the equations that determine the value of n_0, n_1 as,

$$\begin{aligned} \frac{\partial V}{\partial n_0} &= 2\lambda_1 n_0 + \lambda_4 - g \frac{n_1}{\sqrt{n_0}} = 0, \\ \frac{\partial V}{\partial n_1} &= 4\lambda_2 n_1 + 2\lambda_5 - 2g\sqrt{n_0} = 0, \end{aligned} \quad (4.18)$$

where

$$\lambda_4 = V_0 - 2za_s, \quad (4.19)$$

$$\lambda_5 = V_0 - 2za_h. \quad (4.20)$$

Next, we introduce three phase fluctuation fields that represent NG bosons in the FM+2FS phase with $n_0 \neq$

0, $n_1 \neq 0$,

$$\begin{aligned} \Phi_1(x) &= \sqrt{n_0} + i\phi(x), \\ \Phi_2(x) &= \sqrt{n_1} + ib_1(x), \\ \Phi_3(x) &= \sqrt{n_1} + ib_2(x). \end{aligned} \quad (4.21)$$

By substituting Eq.(4.21) into $V(\Phi_\sigma)$ in Eq.(4.16), the quadratic terms of the fluctuating fields are obtained as

$$V_2 = (\phi, b_1, b_2) \begin{pmatrix} 2\lambda_1 n_0 + \lambda_4 & -g\sqrt{n_1} & g\sqrt{n_1} \\ -g\sqrt{n_1} & 2\lambda_2 n_1 + \lambda_5 & -g\sqrt{n_0} \\ g\sqrt{n_1} & -g\sqrt{n_0} & 2\lambda_2 n_1 + \lambda_5 \end{pmatrix} \times \begin{pmatrix} \phi \\ b_1 \\ b_2 \end{pmatrix}.$$

By using Eq.(4.18),

$$\begin{aligned} V_2 &= (\phi, b_1, b_2) \begin{pmatrix} g\frac{n_1}{\sqrt{n_0}} & -g\sqrt{n_1} & g\sqrt{n_1} \\ -g\sqrt{n_1} & g\sqrt{n_0} & -g\sqrt{n_0} \\ g\sqrt{n_1} & -g\sqrt{n_0} & g\sqrt{n_0} \end{pmatrix} \begin{pmatrix} \phi \\ b_1 \\ b_2 \end{pmatrix} \\ &= (\phi, b_1, b_2) g\mathbf{K} \begin{pmatrix} \phi \\ b_1 \\ b_2 \end{pmatrix}. \end{aligned} \quad (4.22)$$

It is straightforward to diagonalize the matrix \mathbf{K} by using a unitary matrix U and obtain the mass gap,

$$U^{-1} \mathbf{K} U = \begin{pmatrix} 0 & 0 & 0 \\ 0 & 0 & 0 \\ 0 & 0 & \frac{2n_0 + n_1}{\sqrt{n_0}} \end{pmatrix}. \quad (4.23)$$

Therefore there are two gapless modes that correspond to the NG bosons, though one may expect three NG bosons as the $U(1)$ pseudo-spin symmetry is spontaneously broken and also both the a and b -atoms Bose condense. From the above derivation of the mass gap, it is obvious that the cubic coupling $g\Phi_1^* \Phi_2 \Phi_3^*$ plays an essentially important role.

The above result can be understood by returning to the original B-t-J Hamiltonian $H_{t,J}$ in Eq.(2.1), and noticing the following correspondence,

$$\Phi_1 \sim S^x - iS^y, \quad \Phi_2 \sim a, \quad \Phi_3 \sim b. \quad (4.24)$$

Furthermore the pseudo-spin \vec{S} is composed of a and b -atoms like $\vec{S}_i = \frac{1}{2} B_i^\dagger \vec{\sigma} B_i$ with $B_i = (a_i, b_i)^t$ in the original B-t-J model. Therefore a global $U(1) \times U(1)$ gauge transformation of a and b -atoms

$$a_i \rightarrow e^{i\theta_a} a_i, \quad b_i \rightarrow e^{i\theta_b} b_i,$$

naturally induces the $U(1)$ transformation of the pseudo-spin,

$$S_i^x - iS_i^y \rightarrow e^{i(\theta_a - \theta_b)} (S_i^x - iS_i^y).$$

This means that the genuine symmetry of the original B-t-J model is not $U(1) \times U(1) \times U(1)$ but $U(1) \times U(1)$. The appearance of the term $g\Phi_1^* \Phi_2 \Phi_3^*$ in the effective field theory eloquently shows this fact. Then the maximum number of the NG bosons is not three but two, as we explicitly demonstrated in the above calculation.

C. Phase diagram and low-energy excitations: Triangular lattice

In this subsection we shall focus on the system on the triangular lattice and study the phase structure and low-energy excitations. The obtained results will be compared with those by the numerical study on the quantum XY model given in the previous section and those of the 3D B-t-J model in the following section. To study the system, we assume a homogeneous state and put $\rho_{1i} = \rho_{2i} = \rho$ ($\rho_{3i} = 1 - \rho_{1i} - \rho_{2i}$). The field Φ_1 represents pseudo-spin degrees of freedom, and it is plausible to assume that its condensation has a uniform amplitude $|\Phi_1| = \text{constant}$ as holes are distributed homogeneously. On the other hand, its phase degrees of freedom has a nontrivial behavior as a result of the frustration. More general cases will be studied in a future publication.

We first study the effective action by a mean-field theory like approximation assuming the $\sqrt{3} \times \sqrt{3}$ symmetry. The triangular lattice is divided into three sublattice labeled A, B and C sublattices. Each field on the sublattice A is denoted as $\Phi_{\sigma A}$ etc. It is not so difficult to search the ground state of the potential. For small a_h (i.e., small t), Φ_2 and Φ_3 do not Bose condensate. On the other hand, a nontrivial long-range order of the pseudo-spin appears for $a_s > V_0$. For constant $|\Phi_1|$, one can show that the state with the three sublattice coplanar order like $\Phi_{1A} = |\Phi_1|$, $\Phi_{1B} = |\Phi_1|e^{i2\pi/3}$, $\Phi_{1C} = |\Phi_1|e^{-i2\pi/3}$ appears as the lowest-energy state. This state obviously corresponds to the phase of the 120° spin order in Fig.4.

To obtain the expectation value of $|\Phi_1|$ and to study low-energy excitations, we relabel the lattice site by dividing it into three sublattices as $i \rightarrow (s, o)$ where $o = A, B$ and C . Then we parameterize the field Φ_1 as

$$\begin{aligned}\Phi_{1A}(s) &= \rho_i \\ \Phi_{1B}(s) &= \rho_i e^{i\frac{2\pi}{3}} \\ \Phi_{1C}(s) &= \rho_i e^{-i\frac{2\pi}{3}}.\end{aligned}\quad (4.25)$$

Effective Hamiltonian of the spin part $H_{\text{eff}}^{\text{spin}}$ is readily obtained from L_{eff} in (4.13) (please notice $a_s < 0$ in the AF case),

$$\begin{aligned}H_{\text{eff}}^{\text{spin}} &= \sum_{i,\mu} \left(|a_s| \Phi_{1i}^\dagger \Phi_{1i+\mu} + \text{c.c.} \right) \\ &+ \sum_i \left(V_0 |\Phi_{1i}|^2 + \lambda_3 |\Phi_{1i}|^4 \right),\end{aligned}\quad (4.26)$$

and substituting Eq.(4.25) into $H_{\text{eff}}^{\text{spin}}$,

$$\begin{aligned}H_{\text{eff}}^{\text{spin}} &= \sum_{i,\mu} \cos \frac{2\pi}{3} \left(|a_s| \rho_i \rho_{i+\mu} + \text{c.c.} \right) \\ &+ \sum_i \left(V_0 \rho_i^2 + \lambda_1 \rho_i^4 \right) \\ &= \frac{|a_s|}{2} \sum_{i,\mu} |\tilde{\nabla}_\mu \rho_i|^2 \\ &+ \sum_i \left(\lambda_1 |\rho_i|^4 - (3|a_s| - V_0) |\rho_i|^2 \right),\end{aligned}\quad (4.27)$$

where $\tilde{\nabla}_\mu$ denotes the difference operator on the triangular lattice.

From Eq.(4.27), Bose condensation of ρ_i takes place for $3a_s > V_0$, and the classical expectation value ρ_{cl} of ρ_i is easily obtained as

$$\rho_{\text{cl}} = \sqrt{\frac{3|a_s| - V_0}{2\lambda_1}}.\quad (4.28)$$

To study the low-energy excitations, we introduce a complex scalar field η_i as follows,

$$\rho_i = \rho_{\text{cl}} + \eta_i,\quad (4.29)$$

and then from Eq.(4.26), we obtain the quadratic terms of η_i in the Hamiltonian as follows

$$H_{\text{eff}(2)}^{\text{spin}} \sim \sum_{\mathbf{k}} \left[\chi(\mathbf{k}) \eta_{\mathbf{k}}^\dagger \eta_{\mathbf{k}} + \beta (\eta_{\mathbf{k}}^\dagger \eta_{-\mathbf{k}}^\dagger + \eta_{\mathbf{k}} \eta_{-\mathbf{k}}) \right]\quad (4.30)$$

where

$$\begin{aligned}\chi(\mathbf{k}) &= -2|a_s| \cos \left(\frac{k_1 a}{2} \right) \cos \left(\frac{\sqrt{3} k_2 a}{2} \right) \\ &- |a_s| \cos k_1 a + \gamma,\end{aligned}\quad (4.31)$$

$$\beta = \lambda_1 \rho_{\text{cl}}^2, \quad \gamma = 4\lambda_1 \rho_{\text{cl}}^2 + V_0.\quad (4.32)$$

We diagonalize Eq.(4.30) by the Bogoliubov transformation and obtain

$$H_{\text{eff}} = \sum_{\mathbf{k}} E(\mathbf{k}) b_{\mathbf{k}}^\dagger b_{\mathbf{k}},\quad (4.33)$$

where

$$E(\mathbf{k}) = \sqrt{\chi(\mathbf{k})^2 - 4\beta^2},\quad (4.34)$$

and its typical behavior is shown in Fig.7. As in the limit $\mathbf{k} \rightarrow 0$,

$$E(\mathbf{k}) \rightarrow 0,\quad (4.35)$$

then $b_{\mathbf{k}}$ represents a NG boson corresponding to the spontaneous symmetry breaking of the U(1) pseudo-spin symmetry.

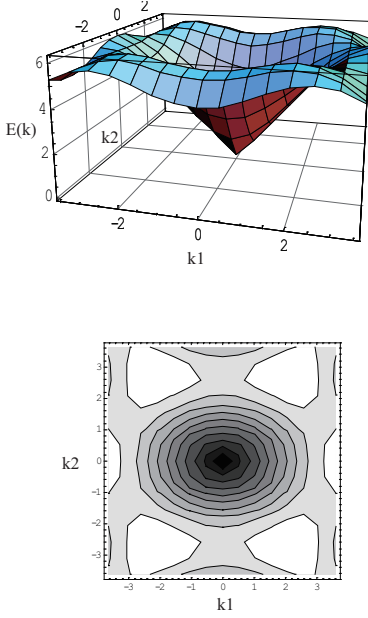


FIG. 7. (Color online) Dispersion relation $E(\mathbf{k})$ in Eq.(4.34). Parameters are $a_s = 1$, $V_0 = 1$, $\gamma = 5$ and $\beta = 1$.

Finally let us study the low-energy excitations in the phase with the 120° spin order *plus* 2SF's that corresponds to the phase B in Fig.4. From Eq.(4.13), the effective Lagrangian $L_{\text{eff}}^{\text{tri}}$ of low-energy excitations in this phase is obtained as

$$L_{\text{eff}}^{\text{tri}} = \sum_i \left(-|a_s| |\nabla \Phi_{1,i}|^2 + a_h |\nabla \Phi_{2,i}|^2 + a_h |\nabla \Phi_{3,i}|^2 \right) - \sum_i \left(\frac{1}{4V_0} |\partial_\tau \Phi_{1,i}|^2 + \frac{1}{4V_0} |\partial_\tau \Phi_{2,i}|^2 + \frac{1}{4V_0} |\partial_\tau \Phi_{3,i}|^2 \right) + V(\Phi_\sigma), \quad (4.36)$$

$$V(\Phi_\sigma) = \sum_i \left[\left(V_0 - 2z|a_s| \right) |\Phi_{1,i}|^2 + \left(V_0 - 2za_h \right) |\Phi_{2,i}|^2 + \left(V_0 - 2za_h \right) |\Phi_{3,i}|^2 \right] - g \left(\Phi_{1,i}^* \Phi_{2,i} \Phi_{3,i}^* + \text{c.c.} \right) + \lambda_1 |\Phi_{1,i}|^4 + \lambda_2 |\Phi_{2,i}|^4 + \lambda_2 |\Phi_{3,i}|^4, \quad (4.37)$$

where z is again the number of links emanating from a single site.

To obtain the ground state, we adopt the following Ansatz for the various condensations, which respects the three-sublattice symmetry,

$$\begin{aligned} \Phi_{1,A} &= \sqrt{n_0}, \Phi_{1,B} = \sqrt{n_0} e^{i\frac{2\pi}{3}}, \Phi_{1,C} = \sqrt{n_0} e^{-i\frac{2\pi}{3}}, \\ \Phi_{2,A} &= \sqrt{n_1}, \Phi_{2,B} = \sqrt{n_1} e^{i\beta}, \Phi_{2,C} = \sqrt{n_1} e^{-i\beta}, \\ \Phi_{3,A} &= \sqrt{n_1}, \Phi_{3,B} = \sqrt{n_1} e^{-i\beta}, \Phi_{3,C} = \sqrt{n_1} e^{i\beta}. \end{aligned} \quad (4.38)$$

The values of n_0 , n_1 and β are determined by substituting Eq.(4.38) into (4.36) and imposing stationary condi-

tion,

$$\begin{aligned} \frac{\partial L_{\text{eff}}^{\text{tri}}}{\partial \beta} &\rightarrow 12a_h n_1 \sin \beta - 4g\sqrt{n_0} n_1 \sin \left(\frac{2\pi}{3} - 2\beta \right) = 0, \\ \frac{\partial L_{\text{eff}}^{\text{tri}}}{\partial n_0} &\rightarrow 2\lambda_1 n_0 + \lambda_4 - g\delta \frac{n_1}{\sqrt{n_0}} = 0, \\ \frac{\partial L_{\text{eff}}^{\text{tri}}}{\partial n_1} &\rightarrow 4\lambda_2 n_1 + 2\lambda_5 - 2g\delta \sqrt{n_0} = 0, \end{aligned} \quad (4.39)$$

where $\delta = \frac{1}{3}(1 + 2\cos(\frac{2\pi}{3} - 2\beta))$. It is verified that non-trivial solutions of n_0 and n_1 exist for sufficiently large a_h and a_s (i.e., negative λ_4 and λ_5). Correlation functions obtained from a typical solution to Eq.(4.39) are show in Fig.8, which have similar behavior to those obtained by the previous MC simulations of the quantum XY model.

As in the square lattice case, we introduce fields that describe low-energy excitations,

$$\begin{aligned} \Phi_{1,A} &= \sqrt{n_0} + i\phi, \\ \Phi_{1,B} &= (\sqrt{n_0} + i\phi) e^{i\frac{2\pi}{3}}, \\ \Phi_{1,C} &= (\sqrt{n_0} + i\phi) e^{-i\frac{2\pi}{3}}, \end{aligned} \quad (4.40)$$

$$\begin{aligned} \Phi_{2,A} &= \sqrt{n_1} + ib_1, \\ \Phi_{2,B} &= (\sqrt{n_1} + ib_1) e^{i\beta}, \\ \Phi_{2,C} &= (\sqrt{n_1} + ib_1) e^{-i\beta}, \end{aligned} \quad (4.41)$$

$$\begin{aligned} \Phi_{3,A} &= \sqrt{n_1} + ib_2, \\ \Phi_{3,B} &= (\sqrt{n_1} + ib_2) e^{-i\beta}, \\ \Phi_{3,C} &= (\sqrt{n_1} + ib_2) e^{i\beta}. \end{aligned} \quad (4.42)$$

Substituting the above equations (4.40), (4.41) and (4.42) into $L_{\text{eff}}^{\text{tri}}$ in (4.36), we obtain the mass term of the fluctuating fields as

$$\begin{aligned} V_2' &= (\phi, b_1, b_2) \begin{pmatrix} g\delta \frac{n_1}{\sqrt{n_0}} & -g\delta \sqrt{n_1} & g\delta \sqrt{n_1} \\ -g\delta \sqrt{n_1} & g\delta \sqrt{n_0} & -g\delta \sqrt{n_0} \\ g\delta \sqrt{n_1} & -g\delta \sqrt{n_0} & g\delta \sqrt{n_0} \end{pmatrix} \begin{pmatrix} \phi \\ b_1 \\ b_2 \end{pmatrix} \\ &= (\phi, b_1, b_2) g\delta \mathbf{K}' \begin{pmatrix} \phi \\ b_1 \\ b_2 \end{pmatrix}, \end{aligned} \quad (4.43)$$

where we have used Eq.(4.39). We can easily diagonalize \mathbf{K}' and get eigenvalues,

$$U^{-1} \mathbf{K}' U = \begin{pmatrix} 0 & 0 & 0 \\ 0 & 0 & 0 \\ 0 & 0 & \frac{2n_0 + n_1}{\sqrt{n_0}} \end{pmatrix}. \quad (4.44)$$

The above result indicates that there are only two NG bosons, though the pseudo-spin $U(1)$ symmetry is spontaneously broken and both the a and b -atoms Bose condense.

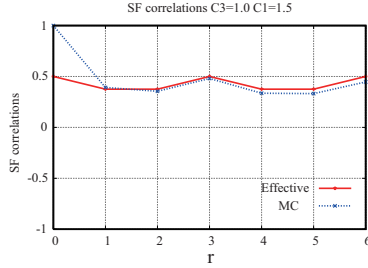


FIG. 8. (Color online) Boson correlation functions $G_{\Phi}(r) = \langle \Phi_{2,i}^* \Phi_{2,i+r} \rangle = \langle \Phi_{3,i}^* \Phi_{3,i+r} \rangle$ in the effective field theory, and $G_a(r) = G_b(r)$, which is numerically obtained in the quantum XY model. We set $n_0 = n_1 = 0.5$, $g = 6$, $a_s = 1$ and $a_h = 1$.

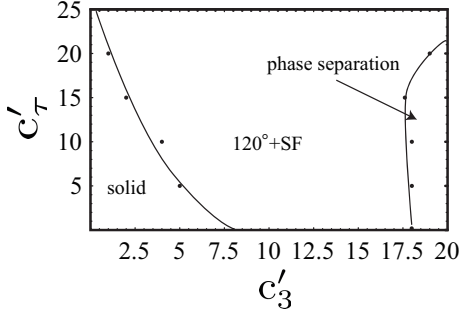


FIG. 9. Phase diagram of the bosonic t-J model in a stacked triangular lattice. $\rho_a = \rho_b = 0.3$, and $C'_1 = 10.0$. System size $L = 18$.

V. PHASE DIAGRAM OF THE BOSONIC t-J MODEL ON STACKED TRIANGULAR LATTICE: NUMERICAL STUDY

In Sec.III.B and IV.C, we studied the low-energy effective theories of the B-t-J model on the triangular lattice at $T = 0$ and obtained phase diagram and low-energy excitations. As we argued previously, if fluctuations of particle density at each site is not so large, the model at $T = 0$ reduces to the system with “Lorentz invariance”, i.e., a linear-time derivative term change to a quadratic-time derivative term¹⁵. In this case, the imaginary time τ plays a similar role to the inter-layer dimension of the stacked 3D lattice.

In the present section, we shall study the B-t-J model on the stacked triangular lattice by numerical simulations with a quasi-classical approximation. Hamiltonian on the stacked triangular lattice is given as follows,

$$\begin{aligned}
 H_{3DtJ} = & - \sum_{\langle r, r' \rangle} t (a_r^\dagger a_{r'} + b_r^\dagger b_{r'} + \text{h.c.}) \\
 & - \sum_r t' (a_r^\dagger a_{r+\hat{z}} + b_r^\dagger b_{r+\hat{z}} + \text{h.c.}) \\
 & + J \sum_{\langle r, r' \rangle} (S_r^x S_{r'}^x + S_r^y S_{r'}^y)
 \end{aligned} \quad (5.1)$$

where $\langle r, r' \rangle$ denotes the NN site of the 2D triangular lattice, and \hat{z} is the unit vector in the inter-layer direction.

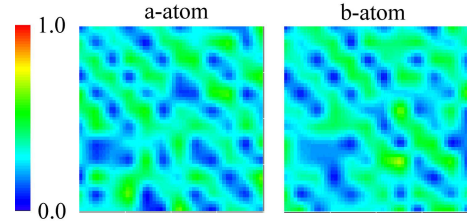
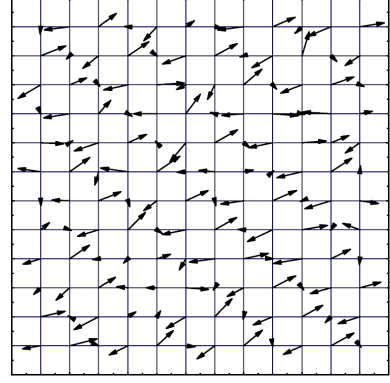


FIG. 10. (Color online) Snapshots of pseudo-spin (upper panel), density of a -atom and b -atom (lower panel). $S^x - S^y$ is the easy plane of the pseudo-spin (see Fig.11), and length of arrows indicates magnitude of the pseudo-spin. A stripe order forms and also there are hole-rich regions. $L = 18$.

There are (at least) two ways of the MC simulation, i.e., the grand-canonical and canonical ensemble. As in the previous studies in this paper, we employ the canonical ensemble with the particle number of each atom fixed. To impose the local constraint, we employ the slave-particle representation (2.2). Then the partition function Z is given as

$$Z = \int [D\phi D\varphi_1 D\varphi_2] e^{-\beta H_{3DtJ}}. \quad (5.2)$$

The path integral in (5.2) is performed by the MC simulation with local update keeping each particle number fixed. We call the calculation (5.2) the quasi-classical approximation as we ignore the Berry phase in the action of the path integral. Some detailed discussion on the validity and physical meanings of this approximation was given in the previous papers²¹.

We first show the phase diagram for $\rho_a = \rho_b = 0.3$ and the hole density = 0.4 in Fig.9, where $C'_\tau = t'/(k_B T)$, $C'_1 = J/(k_B T)$ and $C'_3 = t/(k_B T)$ are all dimensionless parameters. Numerical study was performed for the system size $L = 12$ and 18. For small hopping amplitude t , the system forms a solid with voids whose snapshot is shown in Fig.10. As C'_3 is increased, phase transition to a state with the 120° spin order and 2SF's takes place. In Fig.11, we show the spin and particle correlation functions that verify this conclusion. The previous numerical study of the quantum XY model and

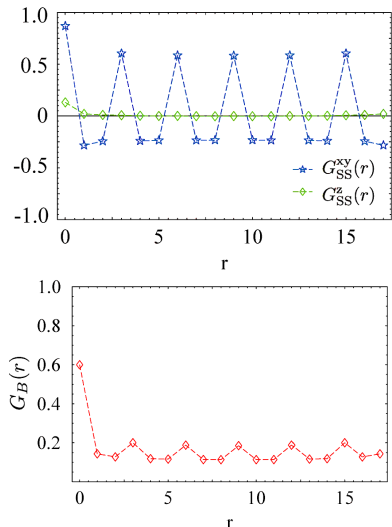


FIG. 11. (Color online) Spin and boson correlation functions obtained by MC simulation of the B-t-J model in a stacked triangular lattice. $C'_\tau = 10.0$ and $C'_3 = 7.0$ in Fig.9. $G_{SS}^z = \frac{4}{L^3} \sum_i \langle S_i^z S_{i+r}^z \rangle$, $G_{SS}^{xy} = \frac{4}{L^3} \sum_{i,a=x,y} \langle S_i^a S_{i+r}^a \rangle$, $G_B(r) = \frac{1}{L^3} \sum_i \langle a_i^\dagger a_{i+r} \rangle = \frac{1}{L^3} \sum_i \langle b_i^\dagger b_{i+r} \rangle$, where sites i and $i+r$ are located in the same 2D triangular lattice. The result indicates the phase with 120° spin order and 2SF's. $L = 18$.

the analytical study by the effective field theory predict the existence of this phase. This result again indicates a strong resemblance of the phase diagram of 2D system at $T = 0$ and that of the corresponding model in stacked 3D lattice. As C'_3 is increased further, phase transition to a phase-separated state takes place. In this phase, the system is divided into a -atom rich region and b -atom rich region, and in each region a SF of single atom forms.

VI. CONCLUSION

In this paper we studied the B-t-J model of the two-component bosons with strong on-site repulsions. We

used the salve-particle representation to treat the local constraint faithfully and derived the effective field theory by integrating out radial degrees of freedom of the slave bosons. The resultant field theory is a kind of extended quantum XY model, and its phase diagram was investigated by the MC simulations. The results shows that the B-t-J model on the square lattice has a simple phase diagram whereas that with the AF pseudo-spin coupling on the triangular lattice has rather complicated structure.

Then we derived the second version of the effective field theory of the B-t-J model by using a ‘‘Hubbard-Stratonovich transformation’’ with the source terms. The resultant field theory describes the pseudo-spin and Bose condensation of the a and b -atoms directly. The effective potential of these order parameters clarifies the phase diagram of the system and verified the existence of the interesting phases like 120° (pseudo-spin)+2SF's on the triangular lattice. Furthermore, we studied low-energy excitations, in particular the NG bosons, in the effective field theory and found that there exist only two NG bosons even in the phase in which the U(1) symmetry of the pseudo-spin is spontaneously broken and the both a and b -atoms Bose condense.

Finally we investigated the B-t-J model on the stacked triangular lattice at finite T by the MC simulations and showed that a similar phase diagram to that of 2D system at $T = 0$ appears. This result means that the direction perpendicular to the 2D triangular lattice plays a similar role to the imaginary-time direction because of the strong on-site repulsion and the spatial lattice structure.

ACKNOWLEDGMENTS

This work was partially supported by Grant-in-Aid for Scientific Research from Japan Society for the Promotion of Science under Grant No23540301.

¹ For review, see, e.g., I. Bloch, J. Dalibard, and W. Zwerger, Rev. Mod. Phys. **80**, 885 (2008); M. Lewenstein, A. Sanpera, V. Ahufinger, B. Damski, A. S. De, and U. Sen, Adv. Phys. **56**, 243 (2008).
² M. Lewenstein, A. Sanpera, and Verònica Ahufinger, ‘‘Ultracold atoms in optical lattices: Simulating quantum many-body systems’’ (Oxford University Press, 2012).
³ D. Jaksch, C. Bruder, J. I. Cirac, C. W. Gardiner, and P. Zoller, Phys. Rev. Lett. **81**, 3108 (1998).
⁴ S. Trotzky, P. Cheinet, S. Fölling, M. Feld, U. Schnorrberger, A. M. Rey, A. Polkovnikov, E. A. Demler, M. D. Lukin, and I. Bloch, Science **319**, 295 (2008).

⁵ A. B. Kuklov and B. V. Svistunov, Phys. Rev. Lett. **90**, 100401 (2003); L. M. Duan, E. Demler, and M. D. Lukin, Phys. Rev. Lett. **91**, 090402 (2003).
⁶ J. Catani, L. De Sarlo, G. Barrontini, F. Minardi, and M. Inguscio, Phys. Rev. A **77**, 011603 (2008).
⁷ E. Altman, W. Hofstetter, E. Demler, and M. D. Lukin, New J. Phys. **5**, 113 (2003).
⁸ S. G. Söyler, B. Capogrosso-Sansone, N. V. Prokof'ev, and B. V. Svistunov, New J. Phys. **11**, 073036 (2009).
⁹ A. Hu, L. Mathey, I. Danshita, E. Tiesinga, C.J. Williams, and C. W. Clark, Phys. Rev. A **80**, 023619 (2009).

- ¹⁰ Y. Nakano, T. Ishima, N. Kobayashi, K. Sakakibara, I. Ichinose, and T. Matsui, Phys. Rev. B **83**, 235116 (2011).
- ¹¹ Y. Nakano, T. Ishima, N. Kobayashi, T. Yamamoto, I. Ichinose, and T. Matsui, Phys. Rev. A **85**, 023617(2012).
- ¹² M. Boninsegni, Phys. Rev. Lett. **87**, 087201 (2001); Phys. Rev. B **65**, 134403 (2002).
- ¹³ It is rather straightforward to treat a_i and b_i as hard-core bosons as in Refs.^{10,11}. As we impose the local constraint excluding the doubly-occupied state in the following calculation, obtained results are qualitatively the same.
- ¹⁴ K. Kataoka, Y. Kuno, and I. Ichinose, J. Phys. Soc. Jpn. **81**, 124502 (2012).
- ¹⁵ S. D. Huber, B. Theiler, E. Altman, and G. Blatter, Phys. Rev. Lett. **100** (2008)050404; L. Pollet and N. Prokof'ev, Phys. Rev. Lett. **109** (2012) 010401.
- ¹⁶ M. Boninsegni and N.V. Prokof'ev, Phys. Rev. **B77**, 092502 (2008); L. He, Y. Li, E. Altman, and W. Hofstetter, Phys. Rev. A **86**, 043620 (2012).
- ¹⁷ N.Metropolis, A.W.Rosenbluth, M.N.Rosenbluth, A.M.Teller, and E.Teller, J. Chem. Phys.**21**, 1087(1953); J. M. Thijssen, "*Computational Physics*", (Cambridge University Press, 1999).
- ¹⁸ K. Sawamura, T. Hiramatsu, K. Ozaki, I. Ichinose, and T. Matsui, Phys. Rev. B **77** (2008)224404; H. Ozawa and I. Ichinose, Phys. Rev. A **86** (2012)015601.
- ¹⁹ S. Doniach, Phys. Rev. B **24**, 5063 (1981); M.P.A. Fisher and G. Grinstein, Phys. Rev. Lett. **60**, 208 (1988).
- ²⁰ See for example, I. Ichinose, Nucl. Phys. **B249**, 715(1985).
- ²¹ K. Nakane, T. Kamijo, and I. Ichinose, Phys. Rev. B **83** (2011)054414; A. Shimizu, K. Aoki, K. Sakakibara, I. Ichinose, and T. Matsui, Phys. Rev. B **83** (2011)064502.